International Conference on Recent Developments in Science, Engineering, Management
YWCA of Delhi, Ashoka Road, Connaught Place, New Delhi (SEM-18)
05th August 2018 www.conferenceworld.in ISBN : 978-93-87793-39-2

Prostate Cancer Detection using 3D Wavelet Analysis

Anil Kumar Prasad[1]

[1]*School of Bio-medical Engineering,National Institute of Technology Kurukshetra, Kurukshetra, India*

ABSTRACT

The motivation behind the paper is to develop strategy for programmed characterization of prostate cancer in light of 3-D wavelet analysis. 3D wavelet analysis is equipped for performing multi resolution analysis under various conditions i.e. it is rotation and direction invariant. The prostate cancer MRIs are decayed utilizing 3D wavelet analysis and the approximation and detail coefficients at every level are utilized as feature vector after dimensionality lessening. Execution of the framework is assessed utilizing two cutting edge classifiers to be specific Support Vector Machine (SVM) and KNN classifier. All examinations are performed on TCIA database, a database for prostate cancer MRIs. We have accomplished promising outcomes with most elevated precision of 100% for SVM classifier and 93.8% for KNN classifier for db4 wavelet function. Some famous existing techniques are likewise assessed for correlation in this paper. The outcome demonstrates that the proposed strategy is more successful and strong than previous techniques. The execution of our framework is great.

***Keywords—* K-Nearest Neighbor (KNN) Classifier, SVM, 3D Wavelet Analysis.**

I.INTRODUCTION

Prostate cancer is one of the main sources cancer related death for men around the world. As of recently, irregular biopsies remain the highest quality level method to identify prostate cancer, yet is intrusive and loose. Radiologists are along these lines investigating the execution of MR imaging joining different MR images to target biopsies towards suspicious regions. Be that as it may, incorporating such a lot of visual data is an unpredictable errand, all the more difficult as prostate cancer and non cancerous tissues may appear to be unique in one MR succession and comparable in another.

A great deal of research work has been finished in this area. Classification of brain tissues utilizing genetic algorithm and support vector machine is proposed. Texture features were extracted from normal and abnormal images using Spatial Gray Level Dependence Method. These extracted features are utilized to train support vector machine classifier for classification purpose. Feature selection for training the SVM classifier is carried out by genetic algorithm.

Brain tumor classification using multiple kernel-based probabilistic clustering (MKPC) and deep learning classifier is investigated. The brain MRI images are segmented using Multiple Kernel based Probabilistic Clustering method. Features are extracted for every segment, and selected using Linear Discriminate Analysis (LDA) method. Deep learning classifier is used for classification into tumor or non-tumor categories. This

paper deals with detection of prostate cancer using 3D wavelet transform, KNN and SVM classifier in the brain MR images.

The organization of this paper is as per the following: Three-Dimensional Wavelet Analysis is detailed in section II. Proposed Methodology is detailed in section III. Experimental Result is detailed in Section IV. Conclusion and Future work is detailed in section V.

II.THREE-DIMENSIONAL WAVELET ANALYSIS

Wavelet transform gives scientific mechanical assemblies to time-scale signal analysis in the comparable route as the short time Fourier transform in the time-frequency domain. The standard differentiation is in the usage of time confined analysing wavelet functions permitting distinctive scale resolution for dilated initial wavelet. Wavelet arrangement worked with two parameters, scale and interpretation give along these lines the capacity to zoom in on the transient behaviour of the signal. The continuous wavelet transform is characterized as the convolution of x(t) with a wavelet function W(t), shifted in time by a translation parameter b and a dilation parameter a (Eq. (1)

$$X_{w(a,b)} = {}^{1}/_{\sqrt{a}} \int_{-\infty}^{\infty} W\left(\frac{t-b}{a}\right) x(t)dt \qquad (1)$$

The discrete type of the wavelet function depends on the discretization of parameters (a, b) on the timescale plane corresponding to a discrete arrangement of continuous functions. This can be accomplished characterizing

$$W_{j,k}\,k(t) = \frac{1}{\sqrt{a_j}} W\left(\frac{t-b_k}{a_j}\right) \qquad (2)$$

for $a_j = a_o^j$ and $b_k = k b_o a_o^j$ where j, k ∈ Z, $a_0 > 1$, $b_o \neq 0$ where j is the dilation and k is the translation. Two prevalent decisions for the discrete wavelet parameters a_o and b_o are 2 and 1 respectively, a setup that is called as dyadic grid arrangement resulting in

$$W_{j,k}(t) = a_0^{-j/2} W\left(a_0^{-j} t - k b_0\right) \qquad (3)$$

$$= 2^{-j/2} W\left(2^{-j} t - k\right) \qquad (4)$$

Wavelet analysis is essentially the route toward decomposing a signal into shifted and scaled forms of a mother wavelet. An basic property of wavelet analysis is impeccable reconstruction, which is the path toward reassembling a decomposed image into its unique form without loss of data. For decomposition and reconstruction, the scaling function $\Phi_{jk}(t)$ and the wavelet $W_{jk}(t)$ are used in the form of

$$\Phi_{jk}(t) = 2^{\frac{-j}{2}} \Phi_0(2^{-j} t - k) \qquad (5)$$

$$W_{jk}(t) = 2^{\frac{-j}{2}}\Psi_0(2^{-j}t - k) \quad (6)$$

where m is dilation or compression and k is translation index. Each basis function w is orthogonal to each basis function Φ.

The one-dimensional wavelet funtion of a discrete time signal $x(n)\ (n = 0,1,\dots,N)$ is performed by convolving signal $x(n)$ with low-pass filter L and high-pass filter H and down sampled by two.

$$c(n)\sum_{n=0}^{L-1} h_0(k)\,x(n-k) \quad (7)$$

$$d(n)\sum_{n=0}^{L-1} h_1(k)\,x(n-k) \quad (8)$$

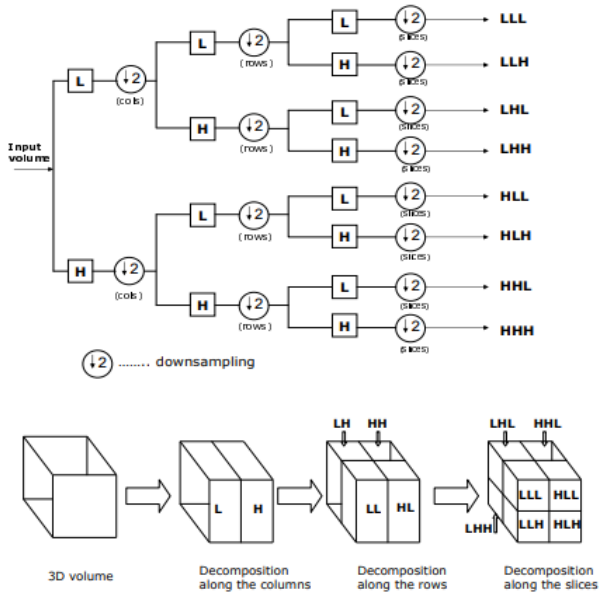

Fig.1 The decomposition tree of the 3D volume structure utilizing discrete wavelet function for columns, rows and slices deliver 8 sub volumes in the primary decomposition stage.

where $c(n)$ represent the approximation coefficients for $n = 0,1,2\dots,N-1$ and $d(n)$ are the detail coefficients, h_0 and h_1, are coefficients of the discrete-time filters L and H respectively.

$$\{h_0(n)\}_{n=0}^{L-1} = (h_0(0), h_0(1), \dots, h_0(L-1)) \quad (9)$$

$$\{h_1(n)\}_{n=0}^{L-1} = (h_1(0), h_1(1), \dots, h_1(L-1)) \quad (10)$$

resulting in the separable, sub-band process.

Comparable decomposition process can be connected for multi-dimensional signals. 3D wavelets can be built as separable products of 1D wavelets by progressively applying a 1D analyzing wavelet in 3 spatial directions (x, y, z). Fig.1 demonstrates a one-level separable 3D discrete wavelet decomposition of an image volume. The volume $F(x, y, z)$ is firstly filtered along the x-dimension, resulting in a low-pass image $L(x, y, z)$ and a high-pass image $H(x, y, z)$. Both L and H are filtered along the y-dimension, resulting in 4-decomposed sub-volumes: LL, LH, HL and HH. Then each of these 4 sub volumes are filtered along the z-dimension, resulting in 8 sub-volumes: $LLL, LLH, LHL, LHH, HLL, HLH, HHL$ and HHH.

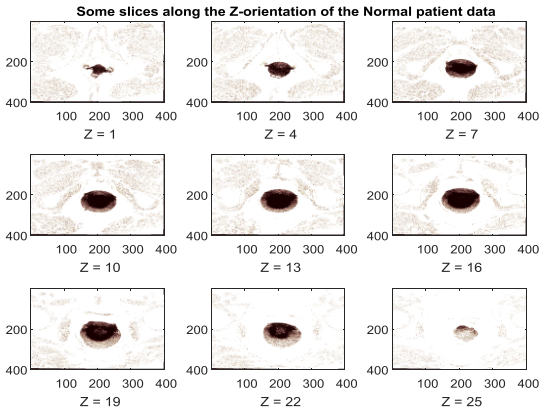

Fig.2 Slices along the Z-orientation of the Normal patient

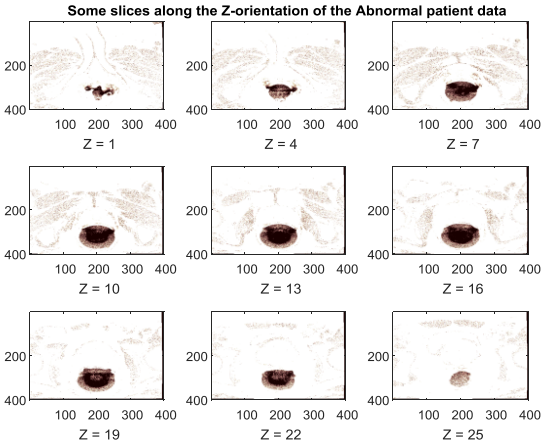

Fig.3 Slices along the Z-orientation of the Abnormal patient

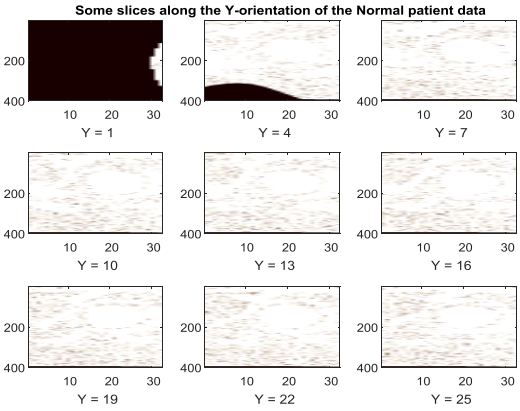

Fig.4 Slices along the Y-orientation of the Normal patient

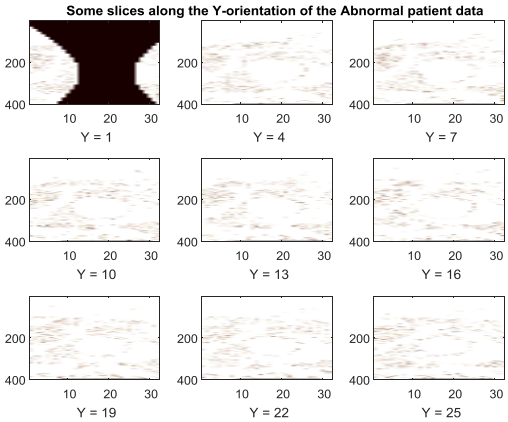

Fig.5 Slices along the Y-orientation of the Abnormal patient

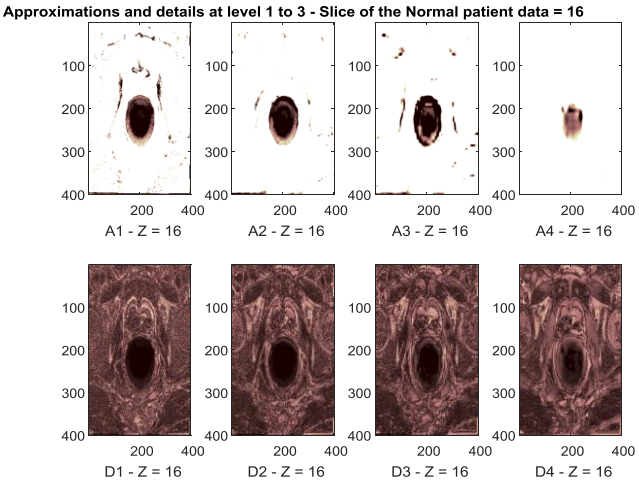

Fig.6 Approximations and details coefficients at level 1 to 3- Slice = 16 of the Normal patient

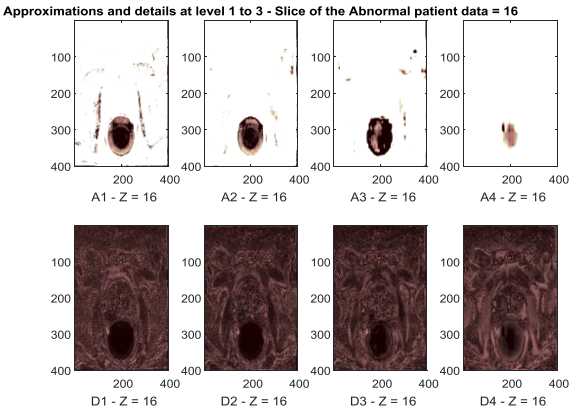

Fig.7 Approximations and details coefficients at level 1 to 3- Slice = 16 of the Abnormal patient

III.PROPOSED METHODOLOGY

A. *TCIA Database*

TCIA database is an open source to encourage examine, advancement and educational activities. We in like manner get our TCIA database with the DICOM pictures from PROSTATE-DIAGNOSIS database. From subject NOs: ProstateDx-01-0020 and ProstateDx-01-0014, we chose all the 32 images from 401-T2WTSEAX-33660 for low risk of prostate cancer in patient (Normal patient Images) and 32 images from 501-T2WTSEAX-00217 for high risk of prostate cancer in patient (Abnormal patient Images).

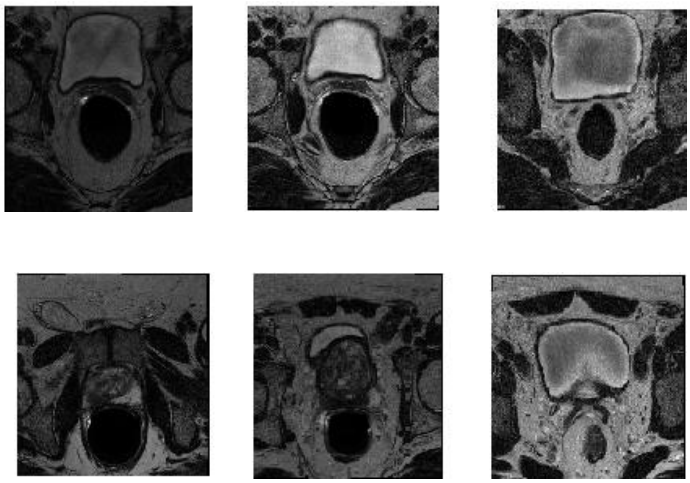

Fig.8 Normal Images (Top row) and Abnormal Images (Bottom row)

In addition, we make group of the prostate images from the PROSTATE-DIAGNOSIS database into 2 classifications in view of our perception without the labels, The 2 classes have 32 and 32 images individually and each image has a similar dimensionality of 400*400 pixels. For this database, it is difficult to group all the prostate cancer images since this is a dynamic database in which images are readied frame by frame with the variation of time. In this way, every one of the images from a similar classification are extremely unique in relation to each other.

B. ***Feature Extraction***

Feature extraction is a crucial factor that impacts the execution of distinguishing proof. In this framework wavelet function (db4) is utilized to extricate feature from MR images. The feature vector got from 4 level wavelet coefficients gives suitable representation for the energy distribution of the signal in time and frequency. The coefficients happen in the entire transmission capacity from low to high frequency. Original signal represented by the sum of coefficients in each sub band.

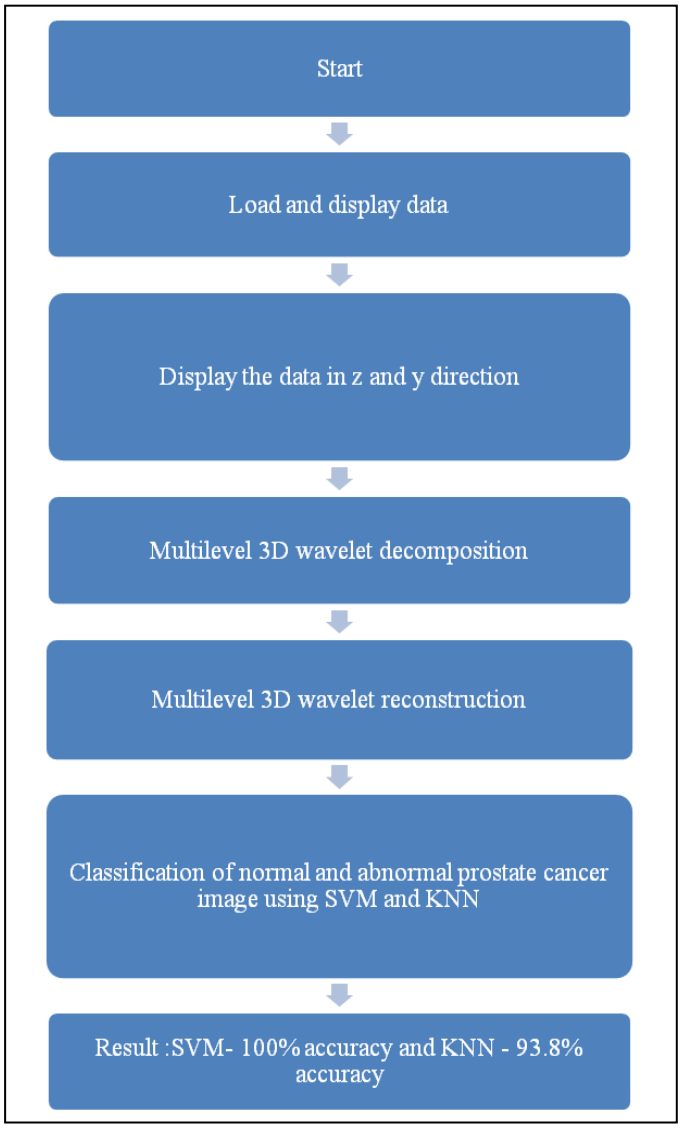

Discrete wavelet transform gives distinctive resolution at different frequency bands by decomposing signal into approximation and detail coefficients at every level. Feature vectors are acquired from the approximation and detail coefficients at 4 levels by the following equations:

1) The mean value of the detail coefficients at every level. These features give frequency distribution data of this signal.

$$\bar{x}_j^d = \frac{\sum |x_j^d|}{n} \qquad (11)$$

Where x_j^d is the detail coefficients at j^{th} level

2) The standard deviation of the detail coefficients at every level. These features gives data about the measure of progress of the frequency distribution.

$$\sigma_j^d = \sqrt{\frac{\sum(x_j^d - \bar{x}_j^d)^2}{n}} \qquad (12)$$

C. ***Feature Matching***

Feature matching was carried out between feature set and query feature utilizing KNN classifier. The training set *s* have *l* points $\{f_1, \ldots \ldots, f_l\}, f_i \in R^n$ and their corresponding class labels are $\{y_1, \ldots \ldots y_N\}$, $y_i \in c, c = \{1, \ldots \ldots, N_c\}$ where no. of different classes are N_c.

Minimum and maximum normalization method was used to standardize the score to typical range between - 1 and 1, going before applying matching procedure. It changed the feature value A to B which lies in the range [-1, 1].

It is given by:

$$B = \left(\frac{A - minimum\ value\ of\ [A]}{maximum\ value\ of\ [A] - minimum\ value\ of\ [A]}\right) \times 2 \qquad (13)$$

SVM classifier is the most efficient algorithm, which utilize the concept of kernel substitution and are known as kernel methods. The training sets of instance-label pairs are given as (x_i, y_i); $i = 1 \ldots \ldots l$ where and $x_i \in R^n$ and $y \in \{1, -1\}^l$ SVM requires the solution of the optimization problem, i.e., the SVM intends to minimize an error function given in equation 14 with the constraint shown in equation 15.

$$\min_{w,b,\xi} \frac{1}{2}\omega^T + C\sum_{i=1}^{l} \xi_i \geq 0 \qquad (14)$$

$$y_i(W^T\emptyset(x_i) + b) \geq 1 - \xi_i, with\ \xi_i \geq 0 \qquad (15)$$

The training vectors x_i is mapped into a higher dimensional space by the function ϕ and in this way SVM finds a straight isolating hyper-plane with the maximal edge in this higher dimensional space $c > 0$, is the parameter of the error term. Also $K(x_i, x_j) \equiv \emptyset((x_i)^T\emptyset(x_j)$ is known as kernel function. By

reducing error function, the SVM learns the extracted feature set effectively in order to categorize the normal or abnormal that are analogous to the training set. From the training data, the SVM classifier learns about the class in which the normal or abnormal is present. Once the SVM is trained, it can classify any prostate cancer MR image dataset in the similar manner. In the classification phase, the selected features that are used in the training process to train the SVM classifier are extracted for testing the prostate cancer image. The feature set is given to the trained SVM for classifying the given prostate cancer MR image.

IV. EXPERIMENTAL RESULT

A medical imaging examination and order system needs outstanding exactness and significant region under the ROC curve to be profitable. So as to assess the accuracy rate dealt with by our structure, we have examined prostate cancer MR images from TCIA dataset of 64 images 32 normal MRI scan images and 32 abnormal prostate cancer MRI scan images. Every 3D MR image was decomposed up to four levels using db4 wavelet function of the prostate cancer MR images and classifying with SVM and KNN classifier. The coefficients acquired at each level after dimensionality reduction, were utilized as feature vectors. The results are averaged from 5-fold cross validation experiments. Classification accuracy of 100% is achieved for SVM classifier and 93.8% is achieved for KNN classifier.

The confusion matrix for different levels of decomposition is given in Figure 9.The Receiver Operating Characteristics (ROC) with various levels of decomposition is shown in Figure 10. Results shows classification accuracy of 100% obtained using the database images.

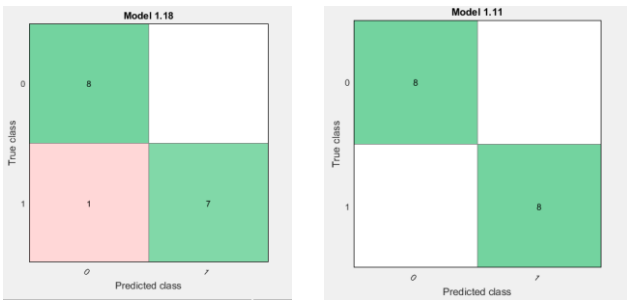

Fig.9 Confusion Matrix for KNN (Left) and SVM (Right)

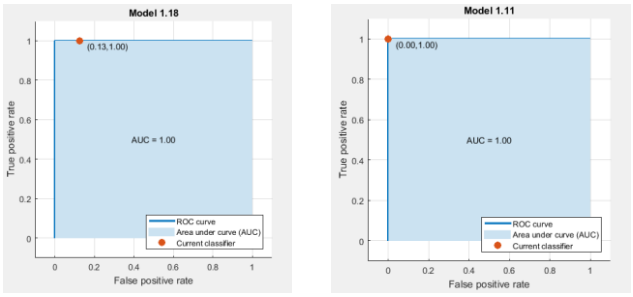

Fig.10 ROC curves for KNN (Left) and SVM (Right)

The system performance with different classifiers are given in table 1.

Table 1. System performance with different classifiers

Classifier	***Accuracy (%)***	***TPR***	***FPR***	***AUC***
Quadratic SVM	100	1.00	0.00	1
Cubic SVM	100	1.00	0.00	1
Fine KNN	100	1.00	0.00	1
Weighed KNN	93.8	1.00	0.13	1

V. CONCLUSION AND FUTURE WORK

This paper proposed a mechanized framework for prostate cancer detection in view of multi-level 3-D wavelet analysis. We applied 3-D wavelet analysis to break down the 3-D MR images up to four levels with a specific end goal to extricate approximation and detail coefficients. Further, features are extricated from approximation and detail coefficients by applying normal insights, for example, mean and standard deviation. The framework was assessed with db4 wavelet function with two distinct classifiers. The proposed system performs magnificently on TCIA dataset with a accuracy of 100% for SVM classifier and 93.8% for KNN classifier. Contrasting the outcomes and different techniques, we can state that the proposed strategy guarantees tremendous potential and that genuine usage should be possible with minimal master supervision in order to classify different types of prostate cancer. In future, this system can be applied to numerous other dataset accessible.

REFERENCES

[1] Clark K, Vendt B, Smith K, Freymann J, Kirby J, Koppel P, Moore S, Phillips S, Maffitt D, Pringle M, Tarbox L, Prior F. The Cancer Imaging Archive (TCIA): Maintaining and Operating a Public Information Repository**,** Journal of Digital Imaging, Volume 26, Number 6, December, 2013, pp 1045-1057.

[2] M. P. Paing and S. Choomchuay, "Classification of margin characteristics from 3D pulmonary nodules," *2017 10th Biomedical Engineering International Conference (BMEiCON)*, Hokkaido, 2017, pp. 1-5.

[3] S. Banerjee, S. Mitra and B. U. Shankar, "Synergetic neuro-fuzzy feature selection and classification of brain tumors," *2017 IEEE International Conference on Fuzzy Systems (FUZZ-IEEE)*, Naples, 2017, pp. 1-6.

[4] É. Niaf, R. Flamary, A. Rakotomamonjy, O. Rouvière and C. Lartizien, "SVM with feature selection and smooth prediction in images: Application to CAD of prostate cancer," *2014 IEEE International Conference on Image Processing (ICIP)*, Paris, 2014, pp. 2246-2250.

[5] M. T. Farooq, A. Shaukat, U. Akram, O. Waqas and M. Ahmad, "Automatic gleason grading of prostate cancer using Gabor filter and local binary patterns," *2017 40th International Conference on Telecommunications and Signal Processing (TSP)*, Barcelona, 2017, pp. 642-645.

[6] R. Trigui, J. Miteran, L. Sellami, P. Walker and A. Ben Hamida, "A classification approach to prostate cancer localization in 3T multi-parametric MRI," *2016 2nd International Conference on Advanced Technologies for Signal and Image Processing (ATSIP)*, Monastir, 2016, pp. 113-118.

[7] A. Firjani *et al*., "A novel image-based approach for early detection of prostate cancer," *2012 19th IEEE International Conference on Image Processing*, Orlando, FL, 2012, pp. 2849-2852.

[8] S. P. Kaulgud, V. R. Hulipalled, S. S. Patil and K. R. Venugopal, "A review on detection of prostate cancer techniques," *2017 International Conference On Smart Technologies For Smart Nation (SmartTechCon)*, Bangalore, 2017, pp. 1189-1194.

[9] S. Banerjee, S. Mitra and B. U. Shankar, "Synergetic neuro-fuzzy feature selection and classification of brain tumors," *2017 IEEE International Conference on Fuzzy Systems (FUZZ-IEEE)*, Naples, 2017, pp. 1-6.

[10] A. Chaddad, P. O. Zinn and R. R. Colen, "Brain tumor identification using Gaussian Mixture Model features and Decision Trees classifier," *2014 48th Annual Conference on Information Sciences and Systems (CISS)*, Princeton, NJ, 2014, pp. 1-4.